Journal of Solid State Chemistry 184 (2011) 3074–3079

Contents lists available at SciVerse ScienceDirect

Journal of Solid State Chemistry

journal homepage: www.elsevier.com/locate/jssc

The first BETS radical cation salts with dicyanamide anion: Crystal growth, structure and conductivity study

N.D. Kushch [a,*], L.I. Buravov [a], A.N. Chekhlov [a], N.G. Spitsina [a], P.P. Kushch [a], E.B. Yagubskii [a], E. Herdtweck [b], A. Kobayashi [c]

[a] Institute of Problems of Chemical Physics RAS, 142432, Chernogolovka, MD, Russia
[b] Technische Universität München, 85747 Garching, Lichtenberg Str. 4, Germany
[c] Department of Chemistry Nihon University, Sakurajosui 3-25-40, Setagaya-Ku, Tokyo 156-8550, Japan

ARTICLE INFO

Article history:
Received 10 June 2011
Received in revised form
30 August 2011
Accepted 5 September 2011
Available online 17 September 2011

Keywords:
Radical cation salts
Synthesis
Structure
Conducting layers
Polymeric anion
Resistivity

ABSTRACT

Electrochemical oxidation of bis(ethylenedithio)tetraselenafulvalene (BETS) has been investigated. Simple and complex dicyanamides of transition metals (Mn^{2+}, Ni^{2+} and Fe^{2+}) were used as electrolytes. The correlation between composition of prepared radical cation salts and metal nature in electrolytes was established. Manganese dicyanamides provide the formation of BETS salts with the $\{Mn[N(CN)_2]_3\}$- and $[N(CN)_2]$-XH_2O anions. When Ni- or Fe-containing electrolytes were used only metalless BETS salts, α''-$BETS_2[N(CN)_2]\cdot 2H_2O$ (**I**) and θ-$BETS_2[N(CN)_2]\cdot 3.6H_2O$ (**II**), formed. Structures and conducting properties of these salts were analyzed. Both salts exhibit layered structure. Conducting radical cation layers have α'' **(I)-** or θ-type (**II**). Anion sheets appear as two-dimensional polymer networks of different types. These networks are formed by $[N(CN)]_2^-$ anions and water molecules interlinked by hydrogen bonds. Salt **I** is a semiconductor and **II** demonstrates resistance drop down to150 K at normal pressure and down to 72 K at ~0.4 kbar pressure.

1. Introduction

In recent years interest has increased in the synthesis and investigation of hybrid multi-functional compounds combining conducting and magnetic properties. Very interesting examples of these are low-dimensional conductors based on radical cation salts of organic π-donors with paramagnetic metal complex ions [1–10]. The structure of these hybrid materials is formed by two subsystems (organic and inorganic) and each manifests different physical properties. Conductivity is associated with π-electrons of organic donor layers, whereas magnetism originates from localized spins of anion layers. A combination of conducting and magnetic properties in crystals of radical cation salts and synergy of these properties results in unique molecular materials and new physical properties. Salts of bis(ethylenedithio)tetrathiafulvalene (BEDT-TTF) and its selenium substituted derivative bis(ethylenedithio)tetraselenafulvalene (BETS) have been of special interest. For example, ferromagnetic metals based on BEDT-TTF [1,2] and antiferromagnetic superconductors based on BETS [7,8] have been prepared. Moreover, magnetic field-induced superconductivity has been found in the λ-$(BETS)_2FeCl_4$ crystals [3,4,7].

In additional to conventional halide, cyanide and oxalate transition metal complexes were used as magnetic counter ions in radical cation salts. In this paper we focus on dicyanamidometallates. These complexes are characterized by a wide variety of structures and different magnetic properties such as ferromagnetism, antiferromagnetism and paramagnetism, which are dependent on type of exchange interactions between unpaired d-electrons of metal atoms through bridging $N(CN)_2$ ligands [11–15]. The character of exchange interactions between unpaired electrons of metal atoms is, in turn, defined by the structures of the salts.

When investigating electrochemical oxidation of BEDT-TTF in the presence of dicyanamides of different metals (Mn^{2+}, Co^{2+}, Cr^{3+} and Cu^{2+}) as electrolytes we found that different products form depending on metal used [15–19]. However, only the use of manganese dicyanamide, $Mn[N(CN)_2]_2$, or a complex salt $Ph_4PMn[N(CN)_2]_3$ resulted in the formation of radical cation salts with dicyanamidometallate anions: $(BEDT\text{-}TTF)_2Mn[N(CN)_2]_3$ [15,19] and $(BEDT\text{-}TTF)_2MnCu[N(CN)_2]_4$ [19]. Recently, we have synthesized the first radical cation salt of BETS with the dicyanamidomanganate(II) anion, k-$BETS_2Mn[N(CN)_2]_3$, which combines superconducting (Tc=5.75 K at P=0.4 kbar) and antiferromagnetic properties [20–21].

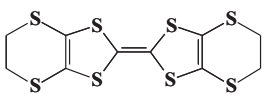

BEDT-TTF

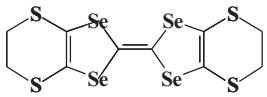

BETS

* Corresponding author.
E-mail addresses: kushch@icp.ac.ru (N.D. Kushch), buravov@icp.ac.ru (L.I. Buravov), anche@icp.ac.ru (A.N. Chekhlov), spitsina@icp.ac.ru (N.G. Spitsina), kpp@icp.ac.ru (P.P. Kushch), yagubskii@icp.ac.ru (E.B. Yagubskii), eberhardt.herdtweck@ch.tum (E. Herdtweck), akoba@chs.nihon-u.ac.jp (A. Kobayashi).

0022-4596/$ - see front matter © 2011 Elsevier Inc. All rights reserved.
doi:10.1016/j.jssc.2011.09.001

Correlations between the metal-dielectric phase transition in the conducting BETS subsystem and the formation of short-range magnetic ordering in the anion layers were found in this salt near metal–insulator transition temperature.

Since the k-$BETS_2Mn[N(CN)_2]_3$ crystals synthesized using the procedure [20] form along with the crystals of another phase and their fraction is not large, we continued our experiments on oxidation of BETS and replaced the solvent and electrolyte used earlier.

We also investigated simple and complex dicyanamide of magnetically active metals: $Ni[N(CN)_2]_2$ and $[(Me_3Ph)P]Fe[N(CN)_2]_3$ as electrolytes. Here we report synthesis, crystal structure and conducting properties of two new BETS dicyanamides, α″-$BETS_2[N(CN)_2]\cdot 2H_2O$ (**I**) and θ-$BETS_2[N(CN)_2]\cdot 3.6H_2O$ (**II**) prepared in the presence of dicyanamides of Ni and Fe, and the synthesis of the k-$BETS_2Mn[N(CN)_2]_3$ crystals grown using the new procedure.

2. Experimental

2.1. Synthesis

2.1.1. Crystals of κ-$BETS_2Mn[N(CN)_2]_3$

The rhomb-like κ-$BETS_2Mn[N(CN)_2]_3$ crystals were synthesized by electrocrystallization of BETS ($C_1=0.12\times10^{-3}$ mol/l) in the benzonitrile (20 ml)—abs. ethanol (2 ml) at constant current $I=0.35$ μA and 25 °C. The complex $(Ph_4P)Mn[N(CN)_2]_3$ salt ($C_2=0.5\times10^{-3}$ mol/l), prepared using the procedure [11], was used as electrolyte.

2.1.2. Crystals of α″-$BETS_2[N(CN)_2]\cdot 2H_2O$

The crystals of α″-$BETS_2[N(CN)_2]\cdot 2H_2O$ (**I**) were prepared in argon atmosphere as black elongated hexagons by electrochemical oxidation of BETS ($C_1=0.25\times10^{-3}$ mol/l) in 1.1.2-trichloroethane (20 ml) to which 10 w/w% of abs. ethanol was added. The reaction was performed at constant current $I=0.3$–0.5 μA at 25 °C using a complex $[(Me_3Ph)P]Fe[N(CN)_2]_3$ salt ($C_2=0.5\times10^{-3}$ mol/l) as electrolyte [22]. The $0.30–0.70\times0.25\times0.05$ mm^3 crystals were grown on a platinum anode for 3 weeks.

2.1.3. Crystals of θ-$BETS_2[N(CN)_2]\cdot 3.6H_2O$ and α″-$BETS_2[N(CN)_2]\cdot 2H_2O$

The θ-$BETS_2[N(CN)_2]\cdot 3.6H_2O$ (**II**) crystals, which appeared as aggregated irregular hexagons with sharing edge, were obtained in a mixture with crystals **I** in argon atmosphere by electrocrystallization of BETS ($C_1=0.25\times10^{-3}$ mol/l) in 1,1,2-trichloroethane (20 ml) to which 10 w/w% of abs. ethanol was added. The reaction was performed at constant current $I=0.5$ μA at 25 °C in argon atmosphere. Electrolyte consisted of a mixture of the $[(Ph)_4P][N(CN)_2]$ and $Ni[N(CN)_2]_2$ salts taken at a 1:1 ratio ($C_2=0.5\times10^{-3}$ mol/l).

2.2. Electron-probe X-ray microanalysis

Preliminary composition of the salts was determined from the electron-probe X-ray microanalysis (EPMA) on a JEOL JSM-5800L scanning electron microscope (SEM) at 100-fold magnification and 20 keV electron beam density. The depth of beam penetration to the sample was 1–3 μm.

2.3. Single crystal X-ray analysis

X-ray analysis of crystals **I** and **II** was performed on a Bruker APEX-II CCD diffractometer (a tube with a rotating anode FR591, graphite monochromator, Mo$K\alpha$ radiation, $\lambda=0.71073$ Å). An array of experimental intensities of the crystals was refined to absorption by multiple use of the SADABS program [23]. The structures were solved by direct method using SHELXS-90 [24] and refined by the full-matrix least-squares method using SHELX-97 [25]. Nonhydrogen atoms were refined in anisotropic approximation. For **I**, parameters of hydrogen atoms of the water molecule were refined in isotropic approximation and the rest hydrogen atoms were set geometrically using the "riding" model.

In the structure of **II** weakly populated and statistically disordered atomic positions of the $[N(CN)_2]^-$ anion and oxygen atoms of the water molecule were revealed in the Fourier synthesis of difference electron density and refined by the full-matrix least-squares method taking into account stoichiometric composition of the salt. Because of weak population of nitrogen and carbon atoms in the anion and oxygen atoms in the water molecule, their parameters were refined in isotropic approximation. For salt **II**, the parameters of all hydrogen atoms were set geometrically.

The main crystallographic data and parameters of structure refinement are presented for both salts in Table 1.

2.4. Resistivity measurements

D.c. measurements were performed using a standard four-probe technique on an automated set in the 300–4.2 K range. Platinum wires 10 μm in diameter were glued to the crystal with DOTITE XC-12 graphite paste.

External pressure was generated by putting the mounted crystal in a drop of silicone oil GKZ-136. Thus, 0.3–0.4 kbar pressure was generated in the sample as a result of the difference between thermal expansion coefficients of the crystal and silicone oil at low temperatures [26].

3. Results and discussion

3.1. Crystal preparation

Electrochemical oxidation of the donor was performed in different solvents such as benzonitrile–absolute ethanol or 1,1,2-trichloroethane–96% ethanol mixtures in the presence of electrolytes comprising simple and complex metal dicyanamides: $(Ph_4P)Mn[N(CN)_2]_3$, $[(Me_3Ph)P]Fe[N(CN)_2]_3$, $(Ph_4P)[N(CN)_2]+Ni[N(CN)_2]_2$. The crystals were identified by EPMA and X-ray analysis.

It is known that the anion sublattice structure in anionic $M[N(CN)_2]_3^-$ complexes depends on a cation, which serves as a molecular template. Depending on nature of the latter, it is formed as chains [11,12], layers [11–14] or three-dimensional networks [14,15]. Thus, the $(Pr_4N)[Mn[N(CN_2)_3]$ salt has a 3D anionic lattice, which is formed as $2\times2\times2$ perovskite superlattice, while that in the $(Bu_4N)Mn[N(CN_2)_3]$ complex is characterized by double bridged (edge-sharing) dimer units, which are further linked by single $N(CN_2)$-bridges to form a 3D network [14]. The salt $(Ph_4P)Mn[N(CN)_2]_3$ [11] has 2D polymeric anion layers similar to insulating layers in k-$BETS_2Mn[N(CN)_2]_3$ [20], which is optimal for k-crystals growth. Neutral $Mn[N(CN)_2]_2$ used as electrolyte in [20] is characterized by 3D rutile-like structure. This is a premise for poor reproducibility of the method because of uncontrolled dissociation of neutral salt, which results in a formation of two phases: k-$BETS_2Mn[N(CN)_2]_3$ and mainly needle-like crystals in electrocrystallization of BETS [20]. Therefore, we substituted $Mn[N(CN)_2]_2$ earlier used by us for $(Ph_4P)Mn[N(CN)_2]_3$. Electrochemical oxidation of BETS in the presence of $(Ph_4P)Mn[N(CN)_2]_3$ in the benzonitrile–abs.ethanol mixture resulted in a preparation of one type crystals only. X-ray analysis of the crystals showed them to be identical to k-$BETS_2Mn[N(CN)_2]_3$. When benzonitrile was replaced by 1,1,2-trichloroethane,

Table 1
Crystallographic data and refined structural parameters for α″-$BETS_2[N(CN)_2]\cdot 2H_2O$ (**I**) и θ-$BETS_2[N(CN)_2]\cdot 3.6H_2O$ (**II**).

	I	**II**
Empirical formula	$C_{22}H_{20}N_3O_2S_8Se_8$	$C_{22}H_{23.2}N_3O_{3.6}S_8Se_8$
Molecular weight	1246.57	1275.40
T, *K*	123(1)	153(2)
Crystal size, mm	0.30 × 0.25 × 0.05	0.33 × 0.15 × 0.03
Crystal system	Monoclinic	Monoclinic
Space group	*P*2(1)/*c*	*P*2(1)/*c*
a, Å	17.506(1)	17.470(2)
b, Å	4.3356(5)	4.2876(5)
c, Å	23.061(2)	11.488(1)
α, deg.	90	90
β, deg.	99.85(1)	98.18(1)
γ, deg.	90	90
V, Å^3	1724.5(3)	851.8(2)
Z	2	1
$\rho_{calcd.}$, g/cm^3	2.401	2.486
μ, mm^{-1}	8.991	9.108
F (000)	1178	605
Total number of reflections	48 857	8576
Number of independent reflections	3113	1554
Number of observed reflections with $I \geq 2\sigma(I)$	2627	1092
Number of refined parameters	256	122
R-factor and *wR* factor for independent reflections	0.0337/0.0745	0.0625/0.0897
R-factor and *wR* factor for observed reflections	0.0256/0.0647	0.0309/0.0568
GOF	1.076	1.052

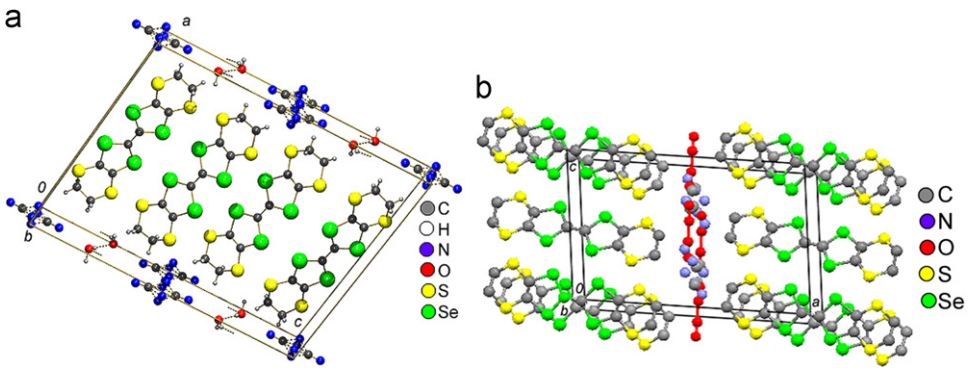

Fig. 1. Crystal structures of the radical cation salts α″-$(BETS)_2[N(CN)_2]\cdot 2H_2O$ (a) and θ-$(BETS)_2[N(CN)_2]\cdot 3.6H_2O$ (b). Dashed lines by oxygen atoms show direction of hydrogen bonds formed between dicyanamide anion and molecule water in the anion sheets.

thin yellowish films grew on the anode. Their composition found from EPMA and conducting properties corresponded to the k-$BETS_2Mn[N(CN)_2]_3$ complex.

Thus, the use of $(Ph_4P)Mn[N(CN)_2]_3$ electrolyte in both solvents provides the formation of a single phase only and a solvent nature strongly affect crystal quality. In contrast to the previously described procedure, the given procedure is well reproducible in benzonitrile and allows preparation of high-quality crystals.

Electrochemical oxidation of BETS in the trichloroethane–ethanol mixture in the presence of mixed electrolyte, $\{(Ph_4P)[N(CN)_2]+Ni[N(CN)_2]_2\}$, results in the formation of a mixture of crystals of **I** and **II**. EPMA showed the absence of nickel in composition of crystals of both types. Composition of crystals was determined by a full X-ray analysis. To understand if the addition of $Ni[N(CN)_2]_2$ affects phase transition of products, we performed electrooxidation of BETS in similar conditions in the presence of $(Ph_4P)[N(CN)_2]$ electrolyte. Crystals of salt **I** only were obtained in these conditions. The addition of $Ni[N(CN)_2]_2$ probably provides the growth of crystals of phase **II**.

Unlike electrolytes used by us only nickel dicyanamide dissolves and dissociates in the trichloroethane-ethanol mixture poorly. This, possibly, is a reason for the formation of crystals **II** together with **I**. It should be noted that during electrocrystalisation several processes can take place: dissolution, dissociation of electrolytes, forming of new metalcomplex anions and growth of crystals of the radical cation salts. Depending on metal nature of complex dicyanamide salts their dissociation often accompay forming of new dicyanamide anions. The combination and competition of these factors often promotes a formation of several crystal phases of BEDT-TTF and BETS salts.

Electrocrystallization of BETS using the $[(Me_3Ph)P]Fe[N(CN)_2]_3$ complex as electrolyte provides formation of crystals whose composition showed no iron as it was determined from EPMA. The crystals were found to be suitable for single-crystal analysis. X-ray analysis showed that crystals prepared using this procedure is salt **I**.

3.2. Crystal structures

Radical cation salts **I** and **II** are characterized by a layered structure in which conducting radical cation layers alternate with inorganic polymer layers formed by dicyanamide anions and water molecules along the *a* axis (Fig. 1a and b).

Crystal structure of **I** is constructed from crystallographically independent BETS radical cations located in a general position, an independent water molecule and an independent half of the $[N(CN)_2]^-$ anion. The anion is located close to the inversion center

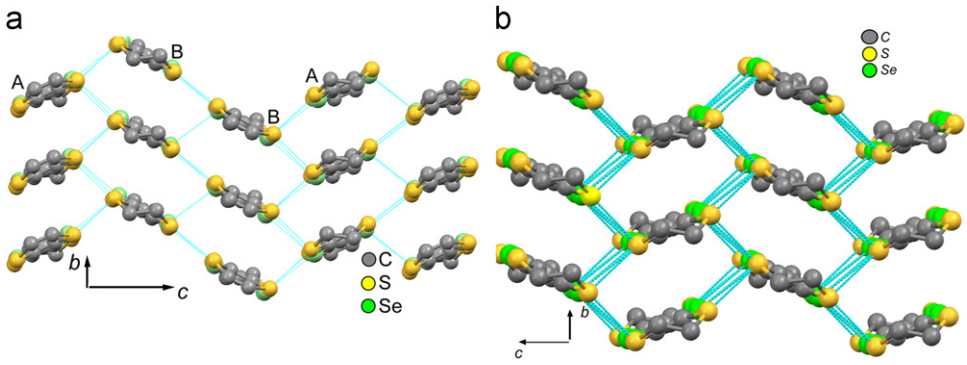

Fig. 2. Radical cation layer in crystals of α″-$(BETS)_2[N(CN)_2]\cdot 2H_2O$ (a) and θ-$(BETS)_2[N(CN)_2]\cdot 3.6H_2O$ (b). Dashed lines show short contact between heteroatoms S and Se.

i (0, 0, 1/2), it is disordered in four positions with 0.32 and 0.18 occupancies. One of the two ethylene groups of the BETS molecule is disordered in the radical cation layer resulting in the appearance of two conformations, "staggered" and "eclipsed", whose ratio is 0.063:0.937 at 123 K. This ratio is 0.15:0.85 in the BEDT-TTF salt isostructural to **I** [16] at room temperature. Disorder in the radical cation layers lowers upon cooling and the share of "staggered" conformation increases.

Crystal structure of salt **II** is constructed from a crystallographically independent half of the BETS radical cation, an independent one-fourth of the $[N(CN)_2]^-$ anion and an independent one-ninth of the water molecule. The radical cation is located at the inversion center *i*(0,0,0). In contrast to **I**, the ethylene groups in the BETS radical cation of salt **II** are ordered and show "staggered" conformation.

The $[N(CN)_2]^-$ anion and water molecules are disordered. Population of nitrogen and carbon atoms in the anion is 0.25 and population of positions of oxygen atoms is 0.5 and 0.4. Disordering of anions and water molecules in the crystal structure of the salt is probably due to two crystal sublattices .The packing mode of ordered radical cations in crystal **II** corresponds to crystal lattice parameters (see Table 1) and packing mode of possibly ordered $[N(CN)_2]^-$ anions and water molecules is probably described in the superlattice with $b' = 4b$.

Conducting layers of α″-type in crystals **I** are built up of stacks A and B of BETS. In stacks of the same type, radical cations are parallel, equidistant (3.98 Å) and transverse-shifted relative to each other. In a radical cation layer, the stacks alternate as -A-B-B-A- with a dihedral angle between average planes of the BETS molecules from stacks A and B (Fig. 2a) is ~127°. Similar values of angles were found in α″-(BEDT-TTF)$_2[N(CN)_2]\cdot 2H_2O$ [16] and α′-$(BEDT\text{-}TTF)_2Cu_5I_6$ [27] isostructural to **I**. Due to shortened contacts between heteroatoms whose value lower than the sum of van-der Waals radii (Table 2), the radical cations from the neighboring stacks form ribbons in the unit cell *c* direction. In addition to shortened S…S, S…Se and Se…Se contacts inside the ribbons, there are similar contacts between radical cations from the neighboring ribbons (Table 2).

Besides mentioned shortened contacts within conducting layers, there is also one shortened S…N contact linking radical cations and dicyanamide groups from the anion layer. The contact value is 3.203 Å.

Radical cation layers of salt **II** are of the θ-type. They are formed by stacks located at an angle of 114.6° to each other (Fig. 2b). The radical cations in the stacks are parallel and the interplanar distance between the neighboring molecules calculated for the atoms of the central TTF fragment is 4.1 Å, which is somewhat higher than that in **I**. Each radical cation in the stack is linked by short S…S, S…Se and Se…Se contacts with the BETS molecules from the neighboring stacks. The values of short contacts between heteroatoms are listed in Table 3.

Table 2
List of short intermolecular contacts in structure of salt α″-$BETS_2[N(CN)_2]\cdot 2H_2O$ (**I**).

Contact	Contact length, Å	Symmetry operation for the 2nd atom in contact
Se1…Se3	3.852 (0.000)	1−*x*, *y*−0.5, 0.5−*z*
Se1…Se3	3.872 (0.000)	1−*x*, *y*+0.5, 0.5−*z*
Se1…S7	3.515 (0.001)	1−*x*, *y*−0.5, 0.5−*z*
Se1…S7	3.658 (0.001)	1−*x*, *y*+0.5, 0.5−*z*
Se2…Se2	3.774 (0.001)	1−*x*, 1−*y*, 1−*z*
Se2…Se2	3.950 (0.001)	1−*x*, 2−*y*, 1−*z*
Se2…Se4	3.700 (0.001)	1−*x*, 1−*y*, 1−*z*
Se2…Se4	3.872 (0.000)	1−*x*, 2−*y*, 1−*z*
Se3…Se3	3.905 (0.001)	1−*x*, *y*−0.5, 0.5−*z*
Se3…Se3	3.905 (0.001)	1−*x*, *y*+0.5, 0.5−*z*
Se4…S6	3.716 (0.001)	1−*x*, 1−*y*, 1−*z*
S5…S7	3.589 (0.001)	1−*x*, *y*−0.5, 0.5−*z*
S5…S7	3.495 (0.001)	1−*x*, *y*+0.5, 0.5−*z*
S6…S8	3.525 (0.001)	1−*x*, 2−*y*, 1−*z*
S8…N1′	3.203 (0.011)	1−*x*, 2−*y*, 1−*z*
H1W…N3′	2.057 (0.018)	*x*, *y*, *z*
H1W…N5′	2.147 (0.016)	−*x*, −*y*, 1−*z*
H1W…N3″	2.086 (0.020)	*x*, *y*, *z*
H1W…N5″	2.139 (0.020)	−*x*, −*y*, 1−*z*
H2W…O0W	1.826 (0.018)	−*x*, *y*−0.5, 0.5−*z*
O0W…N3′	2.826 (0.012)	*x*, *y*, *z*
O0W…N5′	2.993 (0.014)	−*x*, −*y*, 1−*z*
O0W…N3″	2.887 (0.021)	*x*, *y*, *z*
O0W…N5″	2.952 (0.022)	−*x*, −*y*, 1−*z*
O0W…O0W	2.708 (0.006)	−*x*, *y*−0.5, 0.5−*z*

Table 3
List of short intermolecular contacts in structure of salt θ-$(BETS)_2[N(CN)_2]\cdot 3.6H_2O$ (**II**).

Contact	Contact length, Å	Symmetry operation for the 2nd atom in contact
Se1–Se1	3.835 (0.001)	−*X*, −0.5+*Y*, −0.5−*Z*
Se1–Se1	3.835 (0.001)	−*X*, 0.5+*Y*, −0.5−*Z*
Se1–Se2	3.746 (0.001)	*X*, −0.5-*Y*, −0.5+*Z*
Se1–Se2	3.795 (0.001)	*X*, 0.5−*Y*, −0.5+*Z*
Se2–S3	3.560 (0.002)	*X*, −0.5−*Y*, 0.5+*Z*
Se2–S3	3.584 (0.002)	*X*, 0.5−*Y*, 0.5+*Z*
S3–S4	3.553 (0.002)	*X*, −0.5−*Y*, −0.5+*Z*
S3–S4	3.555 (0.002)	*X*, 0.5−*Y*, −0.5+*Z*

The mode of radical cation overlapping in the stacks is similar for both salts. This is so-called RA type [28].

The anion layers in both salts are composed of dicyanamide anions and water molecules (Fig. 3a and b). These layers are of a different type of two-dimensional networks, which are constructed by formation of hydrogen bonds between water molecules and dicyanamide anions.

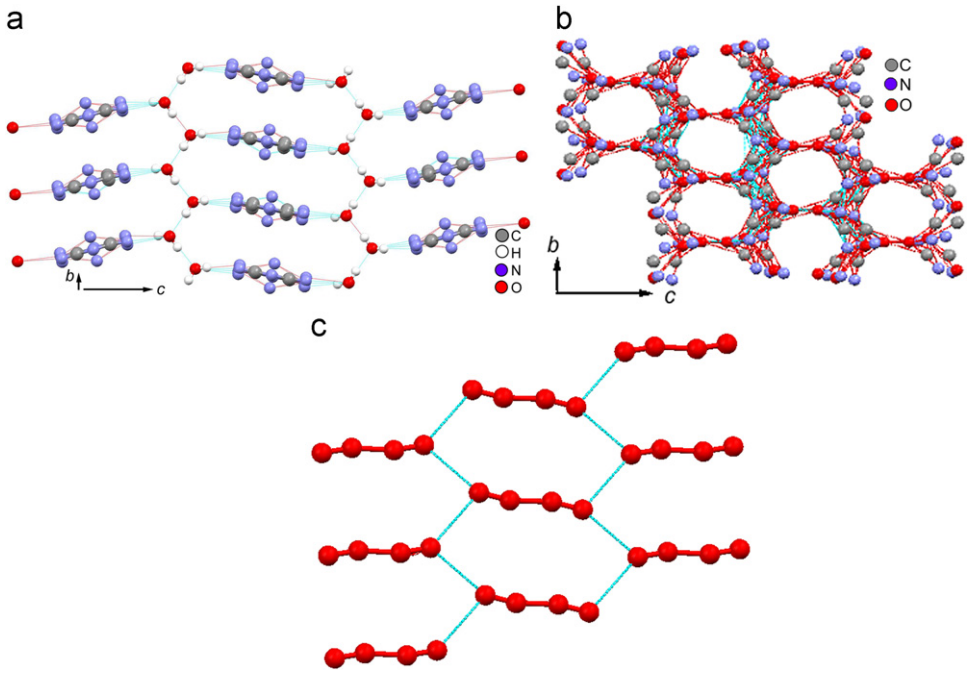

Fig. 3. Anion layer in the crystals of α″-$(BETS)_2[N(CN)_2]\cdot 2H_2O$ (a) and θ-$(BETS)_2[N(CN)_2]\cdot 3.6H_2O$ (b) in *bc* plane. View of the hexagonal polymeric net formed by water molecules in the anion sheets of crystal θ-$(BETS)_2[N(CN)_2]\cdot 3.6H_2O$ (c).

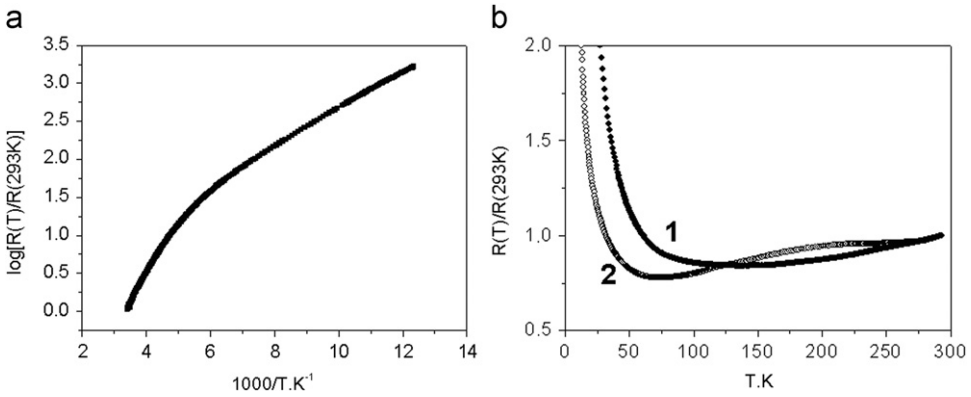

Fig. 4. Temperature dependence of the resistivity measured parallel to conducting radical cation layers for α″-$(BETS)_2[N(CN)_2]\cdot 2H_2O$ (a) and θ-$(BETS)_2[N(CN)_2]\cdot 3.6H_2O$ (b): curve 1—resistivity at ambient pressure and curve 2—under a pressure of ~0.4 kbar created by cooling in GKZ oil.

Hydrogen bonds form along two directions (c и *b* axes) that are distinguishable in the anion layer of salt **I**. In the direction of the *c* axis, hydrogen bonds link hydrogen atoms of the water hydroxyl group to terminal nitrogen atoms of the dicyanamide anion (HW–N or O0W–N). In the transverse direction (along the *b* axis), hydrogen bonds (HW–O0W or O0W–O0W) form by the water molecules only. The values of hydrogen bonds are from 2.057 to 2.147 Å (HW–N) and 2.826–2.952 Å (O0W…N) (Table 2). The values of hydrogen bonds between water molecules are 1.826 (HW–O0W) and 2.708 (O0W–O0W).

Disordered anion layers in salt **II** show a different type of denser packing of the $[N(CN)_2]^-$ anions and water molecules as compared with crystals of **I** (see Table 1**)**. Hydrogen bonds between the $[N(CN)_2]^-$ anions and those between water molecules in **II** form a disordered two- dimensional network (Fig. 3b). Fig. 3c shows a network with dicyanaimde groups excluded for clarity. The network consists of hexagonal honeycomb cells formed by water molecules due to hydrogen bonds between them. Zig-zag chains of disordered dicyanamide anions are built in the network along the *b* axis (Fig. 3b). Unfortunately, because of strongly disordered anions and water molecules, lengths of the formed hydrogen bonds cannot be estimated.

In addition to α″-$(BEDT\text{-}TTF)_2[N(CN)_2]\cdot 2H_2O$ [16] isostructural to **I**, one more radical cation salt of BEDT-TTF with a dicyanamide counter ion, namely, $(BEDT\text{-}TTF)_2[N(CN)_2]$, is known [29]. In contrast to crystals **I** and **II**, anion layers of the latter salt do not involve water molecules and consist of isolated ordered dicyanamide anions only.

3.3. Resistivity measurements

Room-temperature conductivity of crystals **I** and **II** measured in the plane of conducting layers is 0.1–0.5 $\Omega^{-1}\,cm^{-1}$ and 3–5 $\Omega^{-1}\,cm^{-1}$, respectively. With the temperature decrease, **I** shows an exponential dependence of resistivity with activation energy equal to 0.15 eV (Fig. 4a) similarly to that of α″-$(BEDT\text{-}TTF)_2[N(CN)_2]\cdot 2H_2O$.

Fig. 1b shows resistivity temperature dependence measured in the plane of the BETS radical cation layers for the same crystal of salt **II** at normal pressure (curve 1) and under pressure (curve 2). At normal pressure the resistivity of the sample drops to the minimum at 150 K and then slowly grows increasing by 30 times at 4.2 K. Under external pressure of ~0.4 kbar, the growth of resistivity at 4.2 K decreases by approximately 2 times and temperature of the minimum shifts to 72 K. Such behavior of resistivity suggests a high sensitivity of the electronic ground state salt **II** to external pressure. It is known that conducting properties of the many BEDT-TTF and BETS radical cation salts are very sensitive to pressure. In particular, the metal–insulator transition at ~27 K in k-$BETS_2Mn[N(CN)_2]_3$ is suppressed if the sample is cooled in a drop of silicon oil [20] following with a transition to the superconducting state.

It should be noted that no minimum is observed in the $R(T)$ curve at 150 K in some samples **II**. Instead of minimum a weak growth of the resistivity takes place in the range of 300–90 K, followed by a stronger one below 90 K.

4. Conclusion

Electrochemical oxidation of BETS has been investigated in the presence of simple or complex dicyanamide salts of Mn (II), Fe(II) and Ni (II) as electrolytes and a well-reproducible procedure for synthesis of magnetic superconductor κ-$BETS_2Mn[N(CN)_2]_3$ has been developed. The correlation between nature of d-metal involved in the electrolyte molecule and composition and structure of radical cation salts of BETS was determined. It was found that for Mn dicyanamides only, the BETS salt with tri(dicyanamido)manganate anion are obtained, while in the presence of Ni- and Fe-dicyanamide electrolytes BETS is electrooxidized to form two new BETS dicyanamides: α″-$BETS_2[N(CN)_2]\cdot 2H_2O$ (**I**) and θ-$BETS_2[N(CN)_2]\cdot 3.6H_2O$ (**II**). Their crystal structures were determined and conducting properties were investigated. The salts show layered structure in which the conducting radical cation layers of α″- or θ-type in **I** and **II**, respectively, alternate with nonconducting anion sheets. There are several short contacts between S…S, S…Se and Se…Se heteroatoms in the radical cation layers. In **I** one short S…N contact is also present, which links radical cations and dicyanamide groups of the anion sheet. The two-dimensional anionic layers in both salts are composed of $[N(CN)_2]^-$ anions and water molecules linked by hydrogen bonds. However, the layers have different structure. The anion sheet in salt **I** consists of two type chains. Along the *c* axis, the chains are formed by alternating dicyanamide anions and water molecules, and in the perpendicular direction, the chains consist of water molecules only. In salt **II** polymer layer appears as disordered honeycomb network. Salt **I** is a semiconductor. Its room-temperature conductivity is 0.3–0.7 $\Omega^{-1}\,cm^{-1}$. Crystals **II** demonstrate a weak drop of resistivity down to 150 K and a small growth below this temperature. The application of ~0.4 kbar pressure shifts the minimum of the resistivity to 72 K.

5. Supplementary crystallographic data

CCDC 826851 for **I** and CCDC 826852 for **II** contain the supplementary crystallographic data for this paper. These data can be obtained free of charge from the Cambridge Crystallographic Data Centre.

Acknowledgments

This work was supported by the RFBR projects No. 11-02-91338 DFG and the Program of the Russian Academy Science Presidium N18.

Appendix A. Supplementary material

Supplementary data associated with this article can be found in the online version at doi:10.1016/j.jssc.2011.09.001.

References

[1] E. Coronado, P. Day, Chem. Rev. 104 (2004) 5419.
[2] E. Coronado, J.R. Galan-Mascaros, C.J Comez-Garsia., V. Laukhin, Nature 408 (2000) 447.
[3] S. Uji, H. Shinagawa, T. Terashima, T. Yakabe, Y. Terai, M. Tokumoto, A. Kobayashi, A. Tanaka, H. Kobayashi, Nature 410 (2001) 908.
[4] L. Balicas, J.S. Brooks, K. Storr, S. Uji, M. Tokumoto, H. Tanaka, H. Kobayashi, A. Kobayashi, V. Barzykin, L.P. Gorkov, Phys. Rev. Lett. 87 (2001) 067002.
[5] H. Fujiwara, H. Kobayashi, E. Fujiwara, A. Kobayashi, J. Am. Chem. Soc. 124 (2002) 6816.
[6] A. Alberola, E. Coronado, J.R. Galan-Mascaros, C. Gimenez-Saiz, C.J. Comez-Garsia, J. Am. Chem. Soc. 125 (2003) 10774.
[7] H. Kobayashi, H. Cui, A. Kobayashi, Chem. Rev. 104 (2004) 5265.
[8] T. Otsuka, H.B Cui, H. Fujiwara, H. Kobayashi, E. Fijiwara, A. Kobayashi, J. Mater. Chem. 14 (2004) 1682.
[9] G. Saito, Y. Yoshida, Bull. Chem. Soc. Jpn. 80 (2007) 1.
[10] E. Coronado, K.R. Dunbar, Inorg. Chem. 48 (2009) 3293.
[11] J.W. Raebiger, J.L. Manson, R.D. Sommer, U. Geiser, A.L. Rheingold, J.S. Miller, Inorg. Chem. 40 (2001) 2578.
[12] P. Werff, S.R. Batten, P. Jensen, B. Moubaraki, K.S. Murray, R. Robson, E.H.K. Tan, Polyhedron 20 (2001) 1129.
[13] P. Werff, S.R. Batten, P. Jensen, B. Moubaraki, K.S. Murray, Inorg. Chem. 40 (2001) 1718.
[14] J.A. Shlueter, J.L. Manson, U. Geiser, Inorg. Chem. 44 (2005) 3194.
[15] J. Schlueter, U. Geiser, J.L. Manson, J. Phys. IV Fr. 114 (2004) 475.
[16] A.V. Kazakova, N.D. Kushch, A.N. Chekhlov, A.D. Dubrovskii, E.B. Yagubskii, K.V. Van, Russ. J. Gen. Chem. 78 (2008) 6.
[17] (a) E.B. Yagubskii, N.D. Kushch, A.V Kazakova, L.I Buravov, V.N. Zverev, A.I. Manakov, S.S. Khasanov, R.P. Shibaeva, JETP Lett. 82 (2005) 93;
(b) V.N. Zverev, A.I. Manakov, S.S. Khasanov, R.P. Shibaeva, N.D. Kushch, A.V. Kazakova, L.I. Buravov, E.B. Yagubskii, E. Canadell, Phys. Rev. B 74 (2006) 104504.
[18] N.D. Kushch, A.V. Kazakova, L.I. Buravov, A.N. Chekhlov, A.D. Dubrovskii, E.B. Yagubskii, E. Canadell, J. Solid State Chem. 182 (2009) 617.
[19] N.D. Kushch, A.V. Kazakova, A.D. Dubrovskii, G.V. Shilov, L.I. Buravov, R.B. Morgunov, E.V. Kurganova, Y. Tanimoto, E.B. Yagubskii, J. Mater. Chem. 17 (2007) 4407.
[20] (a) Nataliya D. Kushch, Eduard B. Yagubskii, Mark V. Kartsovnik, Lev I. Buravov, Alexander D. Dubrovskii, Anatolii N. Chekhlov, Werner Biberacher, J. Am. Chem. Soc. 130 (2008) 7238;
(b) V.N. Zverev, M.V. Kartsovnik, W. Biberacher, S.S. Khasanov, R.P. Shibaeva, L. Ouahab, L. Toupet, N.D. Kushch, E.B. Yagubskii, E. Canadell, J. Phys. Rev. B82 (2010) 155123.
[21] O.M. Vyaselev, M.V. Kartsovnik, W. Biberacher, L.V. Zorina, N.D. Kushch, E.B. Yagubskii, Phys. Rev. B83 (2011) 094425.
[22] P.M. van der Werff, S.R. Batten, P. Jensen, B. Moubaraki, K.S. Murray, J.D. Cashion, Cryst. Growth Des. 4 (2004) 503.
[23] SADABS (Version 2008/1). Bruker AXS Inc., Madison, Wisconsin, USA, 2008.
[24] G.M. Sheldrick, SHELXS-90. Program for Crystal Structure Determination, University of Göttingen, Göttingen, Germany, 1990.
[25] G.M. Sheldrick, SHELXL-97. Program for Crystal Structure Refinement, University of Göttingen, Göttingen, Germany, 1997.
[26] L.I. Buravov, V.N. Zverev, A.V. Kazakova, N.D. Kushch, A.I. Manakov, Instrum. Exp. Tech. 51 (2008) 156.
[27] L.I. Buravov, A.V. Zvarykina, M.V. Kartsovnik, N.D. Kushch, V.N. Laukhin, R.M. Lobkovskaya, A.V. Merzhanov, D.N. Fedutin, P.R. Shibaeva, E.B. Yagubskii, Zh. Eksp. Teor. Fiz. 92 (1987) 594.
[28] T. Mori, Bull. Chem. Soc. Jpn. 72 (1999) 170.
[29] X. Bu, P. Coppens, Acta Cryst. C48 (1992) 1560.